HHS Public Access

Author manuscript

Microvasc Res. Author manuscript; available in PMC 2020 May 01.

Published in final edited form as:

Microvasc Res. 2019 May ; 123: 7–13. doi:10.1016/j.mvr.2018.11.010.

A simple automated method for continuous fieldwise measurement of microvascular hemodynamics

Sherry G. Clendenon[1,2], **Xiao Fu**[1,3], **Robert A. Von Hoene**[1,2], **Jeffrey L. Clendenon**[4], **James P. Sluka**[1,2], **Seth Winfree**[5], **Henry Mang**[5], **Michelle Martinez**[5], **Adele J. Filson**[5], **James E. Klaunig**[6], **James A. Glazier**[1,2], and **Kenneth W. Dunn**[5]

[1]Biocomplexity Institute, Indiana University, Bloomington, IN, USA

[2]Department of Intelligent Systems Engineering, Indiana University, Bloomington, IN, USA

[3]Department of Physics, Indiana University, Bloomington, IN, USA

[4]Scientific Designs, Indianapolis, IN, USA

[5]Department of Medicine, Indiana University, Indianapolis, IN, USA

[6]School of Public Health, Indiana University, Bloomington, IN, USA

Abstract

Microvascular perfusion dynamics are vital to physiological function and are frequently dysregulated in injury and disease. Typically studies measure microvascular flow in a few selected vascular segments over limited time, failing to capture spatial and temporal variability. To quantify microvascular flow in a more complete and unbiased way we developed STAFF (Spatial Temporal Analysis of Fieldwise Flow), a macro for FIJI open-source image analysis software. Using high-speed microvascular flow movies, STAFF generates kymographs for every time interval for every vascular segment, calculates flow velocities from red blood cell shadow angles, and outputs the data as color-coded velocity map movies and spreadsheets. In untreated mice, analyses demonstrated profound variation even between adjacent sinusoids over seconds. In acetaminophen-treated mice we detected flow reduction localized to pericentral regions. STAFF is a powerful new tool capable of providing novel insights by enabling measurement of the complex spatiotemporal dynamics of microvascular flow.

Keywords

red blood cell velocity; intravital microscopy; hemodynamics; microvascular; capillary

address of corresponding author: Kenneth W. Dunn, kwdunn@iu.edu, Department of Medicine, Indiana University School of Medicine, Research II, Suite E202, 950 W Walnut St, Indianapolis, IN 46202.

[10]Author contributions. The approach was conceived by K.W.D, S.G.C., J.A.G., and X.F. Intravital imaging was performed by S.W., H.M. and M.M. Software was written by X.F., R.A.V.H. and J.L.C. Network skeleton generation was done by S.G.C. and A.J.F. Software and user guide were evaluated and critical input was provided by K.W.D., S.G.C. and J.P.S. Expertise in liver physiology was provided by J.E.K. Manuscript was written by S.G.C. and K.W.D.

[9]Disclosures. The authors report no competing interests.

Subject terms

Basic science research; Hemodynamics; Vascular biology; Imaging

3. Introduction

The microvasculature plays a fundamental role in physiology, ensuring effective tissue perfusion under changing conditions. Since vascular dysfunction underlies some of the most pervasive diseases of the modern world, vascular function has become a primary parameter of interest for a wide range of biomedical investigations. While a variety of techniques are used to evaluate tissue perfusion, only intravital microscopy provides the temporal and spatial resolution necessary to characterize blood flow at the level of individual capillaries in a living animal.

Intravital studies of microvascular function were among the first applications of light microscopy, having been used by van Leeuwenhoek in the late 17th century to observe capillary blood flow in frogs[1]. Microvascular function has remained a primary application of intravital microscopy, with a recent literature search indicating that over 40% of biomedical publications that include the term “intravital microscopy” also include the terms “microvascular” or “microcirculation”.

The most common approach to intravital microscopy of microvascular flow utilizes epi-fluorescence following intravenous injection of fluorescent markers. Studies are then conducted using confocal or multiphoton microscopy (for imaging at depth in tissues) or wide-field epifluorescence (for thin preparations or superficial layers of organs). In either case, speed of microvascular flow necessitates high-speed image collection, typically >60 frames per second (fps). For laser scanning confocal and multiphoton microscopes this speed is generally accomplished only by limiting the field of view, sometimes down to single scan lines. In contrast, even inexpensive wide-field digital microscopes can collect full-frame images at speeds exceeding 100 fps, supporting data collection across entire microscope fields over time. The problem then becomes extraction of the quantitative information contained in the massive image datasets.

Here we describe and demonstrate STAFF, novel software implemented as a macro toolset for the FIJI implementation of ImageJ, that enables efficient analyses of microvascular flow over time throughout entire microscope fields collected at high-speed.

4. Methods

Experimental animal model and surgical procedures

Studies were conducted using 9-10 week-old male C57BL/6 mice (Jackson Labs). Following delivery, animals were acclimated at least 4 days before studies. Surgical preparations were conducted as previously described[2,3]. All animal experiments were approved and conducted according to Institutional Animal Care and Use Committee guidelines of Indiana University, and adhered to the NRC guide for care and use of animals.

Intravital microscopy

Microscopy studies used a Nikon TiE inverted epifluorescence microscope equipped with Nikon Perfect Focus System, Xenon arc lamp, Sutter Lambda 10-3 filter controller and Hamamatsu Orca Flash 4.0 CMOS detector. Images were collected at 97.5 fps, unbinned, at 0.65 μm/pixel (Figures 2,3) or binned 2×2 to 1.3 μm/pixel (Figure 4). All studies used a Nikon Plan Fluor 20X, NA 0.75 multi-immersion objective, water immersion mode. Since the STAFF macro measures microvascular flow in a fixed set of regions, organ stability is crucial. Organ immobilization methods for intravital microscopy are described in our previous publications[2,4]. Field of view may shift briefly during respiration, but returns to its original position after each respiration, allowing reliable measurements.

Obtaining, installing and using the STAFF software

STAFF is a macro written to run in the FIJI distribution of ImageJ[5]. FIJI can be downloaded from https://imagej.net/Fiji#Downloads. and STAFF can be downloaded from https://github.com/icbm-iupui, along with a User's Guide. (The STAFF macro and User's Guide is currently included as Supplemental Material, but will post to the download site after acceptance). The STAFF User's Guide contains step-by-step instructions for installation and use of the STAFF macro and detailed information on parameter selection and interpretation of program output.

Digital image analysis

We conducted digital image analysis using the FIJI implementation of ImageJ. The STAFF macro requires two input files, (1) the time-lapse image sequence and (2) a binary image of the centerlines, or skeleton of the vascular network. Skeletonized images were derived from either a manually generated line drawing of the vasculature or from segmented vasculature. The STAFF User's Guide describes both procedures.

5. Results

An overview of our approach to measuring microvascular flow is presented in schematic form (Figure 1). Following surgical exposure, the organ surface is repeatedly imaged at a high frame rate (Figure 1A). The ability to measure microvascular flow across an entire field requires collection of images of the field at rates sufficient to resolve an individual red blood cell's (RBC's) trajectory in space-time kymograph images of individual vessel segments. Under ideal circumstances, the fastest speed that can be resolved in a kymograph is one in which an RBC shadow is displaced by one unit of time (one pixel) over the length of the segment. Thus, the maximum measurable speed is a function of both frame rate and segment length, with a theoretical upper limit being the product of segment length and frame rate. However, this limit pertains to ideal data; in practice, approaching this limit depends upon the signal-to-noise ratio in the images.

For most applications, frame rates required for measuring microvascular flow can only be accomplished with field-imaging systems such as wide-field or spinning disk confocal microscopy. Although resonant scanning systems support image capture at 30 fps, for most samples, image quality is poor at these rates. Even in the best case, measurements of RBC

velocities in the range of the highest rates previously reported, nearly 2000 μm/sec[6], would be limited to segments more than 66 microns in length, significantly longer than a large fraction of sinusoid network segments.

In our preliminary studies of mouse liver microvasculature labeled with fluorescent dextran, we compared image series collected at 30, 60, 100 and 200 fps. We found the best trade-off between segment length and signal-to-noise was obtained when image collection was conducted at 100 fps, which provides the theoretical capability to measure velocities up to 2000 μm/sec in segments as short as 20 microns. In our studies in mouse liver, RBC velocities over 1000 μm/sec were seldom observed.

We analyze flow velocities for every vascular segment in the image field over multiple time intervals throughout the period of the video. Vascular segments are identified as the lengths of vasculature between branch points or terminating in a free end (point where a vessel leaves the image plane). Time intervals are specified by the user; here we specify time intervals as the period during which the image remains steady between short periods of motion that commonly occur during respiration (Figure 1B, white arrows). The region-of-interest (ROI) that represents each vascular segment is obtained by skeletonization of either a line drawing or segmented vasculature (Figures 1C and STAFF User's Guide Sections on Additional Information about Analyze Skeleton and generating skeleton files, Hand editing simple networks, and Supplemental Figure 17). STAFF then analyzes the skeleton [7] assigning a unique identifying number to each segment and saving it in an ROI manager file along with the line drawing of that ROI and its spatial location.

For each vascular segment over each time interval, STAFF creates a kymograph by plotting intensity from the original image sequence along the ROI (Figure 1B, middle panel, yellow box) for all images of that time interval. RBC flow along that line segment is visible in the kymograph as light and dark angled lines that correspond to RBC distance traveled (d) and time elapsed (t). Using the Directionality plugin in FIJI [8], angles in the kymograph are detected and a histogram is produced with a peak at the dominant orientation (Figure 1B,C). A Gaussian distribution is fitted to the highest peak in the histogram and the angle at the center of the distribution is reported. From this angle and the spatial and temporal calibration for the image, STAFF calculates RBC flow velocity along that vascular segment. STAFF then generates a spreadsheet file containing all segment velocities for each time interval, supporting examination and quantitative analysis in separate statistical analysis software. STAFF also generates a color-coded velocity map for each time interval that can be viewed as a time sequence or as a 3D volume, allowing intuitive visual exploration of the full spatiotemporal dataset.

The major value of STAFF lies in its ability to efficiently quantify microvascular flow in large and complex networks collected over extended periods of time. While microvascular flow can be measured manually, the time required to analyze a single kymograph representing one vascular segment over one time interval (~5 minutes for manual kymograph analysis, or ~30 minutes for tracking individual cells) is such that manual approaches are practical only for analyses of small numbers of vascular segments over limited periods of time. For analyses of the kinds of microvascular networks shown here,

which consist of 300-500+ segments imaged over 30-100+ time periods, manual kymograph analysis could require over a year at 40 hours per week, and manual tracking analysis could take over 7 years. In contrast, STAFF completes this analysis in less than a day.

Measurements of RBC velocity in the microvasculature of the mouse liver

Using STAFF, we analyzed microvascular flow in the mouse liver (Figure 2). A mouse was placed on the stage of a wide-field microscope following intravenous injection with fluorescein dextran and surgical presentation of the left lobe of the liver. Following equilibration, a series of fluorescence images was collected over three minutes at 97.5 fps. Resulting data (~18,000 images) were then analyzed using STAFF. The first twenty seconds of the time series is depicted as a volume with time represented as depth (Figure 2A). Inspection of the first ten seconds of this time series (Video1, plays 1/3rd actual speed), show that profound variability exists in hepatic microvascular flow. Sinusoidal segments with vigorous flow can be found immediately adjacent to segments where flow has completely stopped, with higher flow rates overall in pericentral regions. This spatial variability is particularly apparent in the color-coded velocity map (Figure 2B). This time series also demonstrates surprising amounts of temporal variability in microvascular flow, with flow in an individual segment changing dramatically, or even stopping and restarting, over seconds. This temporal variability is apparent when velocity maps for each inter-respiratory interval are evaluated in time series (Video 2), or as volume renderings (Figure 2C).

STAFF also provides velocity measurements for all segments over all time intervals in a spreadsheet, which can be further summarized and analyzed. The mean of all velocities in the field over the 3-minute period of image collection was 325.02 μm/sec (s.e.m. 2.01, n=25489) a value that was stable over time. We also plotted a histogram for all segments over all time intervals during the 3-minute period of image collection (Figure 2D). This histogram demonstrated a bimodal distribution of velocities; one in the range greater than zero but less than 100 pm/sec and a second, broader distribution of values centered around 450 μm/sec. This bimodal distribution of velocities is similar to the velocities distribution predicted from simulations of blood flow in model liver lobules[9]. When velocities from individual segments are plotted as a function of time interval, velocity changes in individual segments over time can be evaluated. Examples are shown of a segment maintaining a high rate of flow throughout the time series and a segment with relatively turgid flow punctuated by occasional stoppages (Figure 2E) and of two sinusoidal segments whose velocities sum to the velocity of the single downstream segment into which the two flow (Figure 2F).

The process of analyzing this volume demonstrated a few features of the analysis process that may need particular scrutiny. First, the quality of the region-of-interest map is critical. Since images are collected from a single focal plane in a 3-dimensional network, some apparently simple segments may contain hidden nodes where undetected vessels connect from above or below. Such segments are characterized either by bidirectional flow, emanating away from or converging towards the node, or by a change in flow velocity at the node. Measurements obtained from such segments thus misrepresent the flow of one or the other contributing segments. Since the direction and magnitude of flow are identified from the most prominent angle in the kymograph, small shifts in the image field can cause the

detected maximum to spuriously shift between the velocities of the two contributing segments. These problems can be avoided by carefully evaluating the region-of-interest map prior to STAFF analysis. Furthermore, since STAFF provides each segment with an identifying number that is listed in both the spreadsheet and the region-of-interest map, interesting or aberrant behaviors of individual segments can (and should) be evaluated after analysis.

Stability of organ preparation is critical. The investigator must prevent lateral tissue displacement and also ensure tissue stability relative to the plane of focus. Since vascular segments occupy different depths in tissue, even subtle changes in focus can compromise imaging of a few segments in a field. Indeed, in the study described above, inspection of the velocity map uncovered a segment whose flow rates appeared to fluctuate between 0 and 1000 μm/sec, before stopping altogether. Inspection of the time series demonstrated that this apparent loss of flow reflected the point at which this segment departed the focal plane of the objective. (This later interval was omitted from data presented in Figure 2). Subtle changes in focus can be difficult to detect visually, and since they may affect only a small fraction of vascular segments may likewise be difficult to detect in measured results. However, the tools provided by STAFF for inspection of individual segments make it relatively simple to identify and evaluate questionable segments.

It was critical to us to be able to use the same skeleton over the entire period of analysis to give us the ability to examine data from individual segments over time. Thus, we limited our analyses to inter-respiratory periods where the field returned to the same location after respiration. For fields with just a small x,y drift over time images can simply be repositioned in x,y. Our tests of image registration by cross-correlation frequently failed, presumably because of the large displacement during respiration and the high proportion of the image that was in motion in inter-respiratory periods. Ultimately, even with these limitations, STAFF returned more data over a larger area over a longer period of time than was possible without STAFF.

Validation of STAFF measurements of RBC velocities

We verified the accuracy of the measurements obtained from STAFF by comparing them with results obtained by manually tracking individual RBCs and by manually evaluating kymographs. We performed manual analyses for every tenth segment from the first time interval from the dataset shown in Figure 2. The validation measurements were done blind, without knowledge of the corresponding STAFF measurements. STAFF measurements of RBC velocities closely agree with velocities obtained by either manual method (Figure 3). We also qualitatively verified STAFF results (for the first time interval) by visually comparing flow of every segment to measurements obtained from STAFF. Visual assessment of whether flow speed in a segment was fast, medium, slow or stopped (defined as velocities < 1 μm/sec) agreed well with STAFF analysis. STAFF velocities did not match visual assessment in 2 segments out of 334. The first anomaly was caused by a region-of-interest that was misplaced over the edge of a vessel, and the second reflected a vessel that was out-of-focus.

STAFF analysis of the effects of acetaminophen on microvascular flow in the mouse liver

Previous studies demonstrated that acetaminophen (APAP, or Paracetamol) acutely alters microvascular flow in mice liver, quantified as the fraction of perfused sinusoids per microscope field[10,11]. APAP hepatotoxicity occurs primarily in centrilobular liver regions suggesting that effects of APAP on microcirculatory flow might likewise manifest in the regions immediately surrounding the central veins.

To test the ability of STAFF to detect such localized effects, we applied the techniques described above to studies of mice four hours after intraperitoneal injection of 250 mg/kg acetaminophen or vehicle. Treatment with vehicle had no apparent effect on appearance of the liver microvasculature, which, similar to Figure 2, shows relatively homogenous distribution of fluorescent dextran throughout the microvasculature (Figure 4A) with minor accumulation around the portal regions. In contrast, fluorescent dextran appears to accumulate in regions surrounding the central veins in a mouse treated with APAP (Figure 4B). Consistent with this appearance, comparison of microvascular flow in time-series images from vehicle and APAP-treated mice demonstrate profoundly reduced pericentral microvascular flow in the APAP-treated mouse (Video3).

The qualitative impression that APAP reduces microvascular flow in pericentral regions is supported by quantitative STAFF analysis. Whereas pericentral vessels show some of the highest velocities in the field in a vehicle-treated animal, in APAP treated mice pericentral vessels are characterized by turgid flow (Figures 4C,D). When integrated across the entire field over a period of one minute, effects of APAP appear subtle. APAP treatment reduced mean RBC velocity from 359 to 314 μm/sec (4.07 s.e.m., n=5934; 5.17 s.e.m., n=4087) an effect that appears to largely result from increasing the percentage of segments with velocities of 0-100 μm/sec (Figures 4E and 4F). However, with analysis restricted to pericentral vessels, the effect of APAP becomes more apparent. Figures 4G and 4H show the results of analysis of eight pericentral segments from the circled regions of Figures 4C and 4D, respectively. In this pericentral region, APAP reduced RBC velocity from 483 to 193 μm/sec (s.e.m. 23.7, n=357; s.e.m 22.3, n=143) and increased the percentage of segments with velocities between 0-100 μm/sec from 35% to 70%.

6. Discussion

Intravital studies have been conducted using wide-field microscopy for hundreds of years. Recent studies increasingly turn to laser scanning confocal or multiphoton systems, whose capability to eliminate out-of-plane fluorescence and (in multiphoton microscopy) to penetrate deep into scattering tissues is better suited to imaging intact, living tissues. However, the low frame rate of raster-scanning systems, generally limits studies of microvascular flow to measurements of single capillaries[12-16]. Clever approaches developed to compensate for the slow rate of image capture in raster scanning systems support measurement of microvascular flow throughout a field[17-19] but are limited in their capability to continuously monitor microvascular flow.

Although wide-field microscopy is compromised by poor rejection of out-of-focus fluorescence, even inexpensive systems can collect images at hundreds of fps. This high

speed makes them uniquely capable of continuously monitoring flow throughout a two-dimensional microvascular network in thin tissues such as the mesentery, or at the surface of organs. Multiple approaches exist to measure RBC velocities in wide-field intravital images of microvascular flow that are typically based upon measuring displacement of RBC shadow in microvasculature labeled with fluorescent dextran or fluorescently labeled cells. RBC velocities are then generally quantified utilizing either cross-correlation analysis of image sequences[20-23] or measurement of the angles of RBC shadows in space-time images derived from image sequences[24-26].

However, none of these approaches exists in a form that is easily implementable by most biomedical researchers for more than a limited number of selected segments per animal. For this reason, we developed STAFF. Designed for two-dimensional images collected at high rates (~100 fps), STAFF image processing and analysis workflow is implemented in a FIJI macro toolset, providing investigators with a simple-to-use approach for automatically measuring microvascular network flow continuously across an entire image field. STAFF expedites extraction of rich information that is latent in high-speed time series images of the microvasculature. In the proof-of-principle studies shown here, STAFF exposed hitherto unobserved levels of spatial and temporal variability in microvascular flow in mouse liver.

As discussed previously, measurements of microvascular flow depend upon the quality of the time-series images. In addition to signal-to-noise ratio, flow measurements are susceptible to the effects of periodic image “flicker”, from contamination by external light sources or from instability in epi-illumination, encountered in lamps reaching the end of their useful lifetime. Even if the angle produced by RBC flow in kymographs is obvious to the human eye, periodic flicker produces horizontal bands in kymographs, resulting in directionality values at zero degrees. If the zero angle peak is the major peak, the directionality plugin reports a value very near zero degrees, resulting in velocity measurements that are impossibly high. If the zero angle peak is not the major peak, it still influences curve fit and shifts results towards higher velocities. To address this problem, STAFF provides the option to ignore angles occurring at zero degrees (“Flicker correction”). Close inspection of Video3 shows that the images collected to studies the effects of acetaminophen were compromised by lamp flicker. Evaluations of histograms generated with and without flicker correction demonstrated that the flicker correction option was effective at removing artifactual values from the directionality histograms without affecting legitimate angle measurements (Supplementary Figure 20).

While powerful, this approach is limited in a few respects. First, like any form of intravital microscopy, data is captured from a limited region of an organ, typically tens of microns deep and less than a millimeter in diameter. Caution must be employed extrapolating from such small regions. Second, data is captured for a single plane, providing a limited window into the underlying three-dimensional microvascular network. Flow in three-dimensional networks can be characterized by combining images collected in time series from different focal planes[23,25], or from different orientations and scan speeds[18]. However, data from different regions that are not collected contemporaneously may generate inaccurate three-dimensional flow maps in systems with significant temporal variability. Light sheet microscopy, a high speed optical sectioning method, is capable of three-dimensional image

capture fast enough to characterize the heartbeat of zebrafish embryos[27], but the geometry of these systems are generally incompatible with imaging mammalian organs in vivo.

Despite these limitations, this approach has provided us with unique insights into the dynamics of microvascular flow in mouse liver that, in some ways, require a rethinking of how we measure microvascular flow. The spatial and temporal variability detected here demonstrate that overall characterizations of microvascular flow cannot be based upon measurements obtained from a few capillaries at a single time point, but rather require measurements obtained from capillary networks, obtained over time, ideally across multiple time scales. The raw data necessary for continuous measurement of microvascular flow throughout a two-dimensional network can be easily obtained using wide-field microscopy. The STAFF image analysis workflow provides an indispensable tool that greatly simplifies the daunting task of converting raw data of this volume and complexity into quantitative data that can be evaluated and interpreted.

Supplementary Material

Refer to Web version on PubMed Central for supplementary material.

Acknowledgments.

Microscopy studies were conducted at the Indiana Center for Biological Microscopy. We thank Dr. Gosia Kamocka for technical assistance with microscopy.

8. Sources of funding. Studies presented here were supported by funding from the National Institutes of Health (U01 GM111243).

Non-standard abbreviations and acronyms:

STAFF	Spatial Temporal Analysis of Fieldwise Flow
FIJI	FIJI Is Just ImageJ
RBC	Red blood cell
APAP	Acetaminophen (Paracetamol)
ROI	Region of interest
fps	frames per second
μm/sec	microns per second

11. References

1. Van Leeuwenhoek A Microscopical observations concerning blood, milk, bones, the brain, spittle, and cuticula. Philos Trans 9, 121–128 (1674).
2. Dunn KW & Ryan JC Using quantitative intravital multiphoton microscopy to dissect hepatic transport in rats. Methods 128, 40–51, doi:10.1016/j.ymeth.2017.04.015 (2017). [PubMed: 28434905]
3. Babbey CM et al. Quantitative intravital microscopy of hepatic transport. IntraVital 1, 44–53, doi: 10.4161/intv.21296 (2012).

4. Dunn KW, Sutton TA & Sandoval RM Live-Animal Imaging of Renal Function by Multiphoton Microscopy. Curr Protoc Cytom 83, 12.19.11–12.19.25, doi:10.1002/cpcy.32 (2018).
5. Schindelin J et al. Fiji: an open-source platform for biological-image analysis. Nat Methods 9, 676–682, doi:nmeth.2019 [pii]10.1038/nmeth.2019 (2012). [PubMed: 22743772]
6. Sherman IA, Pappas SC & Fisher MM Hepatic microvascular changes associated with development of liver fibrosis and cirrhosis. Am J Physiol 258, H460–465, doi: 10.1152/ajpheart.1990.258.2.H460 (1990). [PubMed: 2309911]
7. Arganda-Carreras I, Fernandez-Gonzalez R, Munoz-Barrutia A & Ortiz-De-Solorzano C 3D reconstruction of histological sections: Application to mammary gland tissue. Microsc Res Tech 73, 1019–1029, doi:10.1002/jemt.20829 (2010). [PubMed: 20232465]
8. Liu ZQ Scale space approach to directional analysis of images. Appl Opt 30, 1369–1373 (1991). [PubMed: 20700292]
9. Fu X et al. Modeling of xenobiotic transport and metabolism in virtual hepatic lobule models. PLoS ONE 13(9): e0198060 10.1371/journal.pone.0198060 (2018). [PubMed: 30212461]
10. Ito Y, Bethea NW, Abril ER & McCuskey RS Early hepatic microvascular injury in response to acetaminophen toxicity. Microcirculation 10, 391–400, doi:10.1038/sj.mn.7800204 (2003). [PubMed: 14557822]
11. Ito Y, Abril ER, Bethea NW & McCuskey RS Role of nitric oxide in hepatic microvascular injury elicited by acetaminophen in mice. Am J Physiol Gastrointest Liver Physiol 286, G60–67, doi: 10.1152/ajpgi.00217.2003 (2004). [PubMed: 12969830]
12. Chhatbar PY & Kara P Improved blood velocity measurements with a hybrid image filtering and iterative Radon transform algorithm. Front Neurosci 7, 106, doi:10.3389/fnins.2013.00106 (2013). [PubMed: 23807877]
13. Drew PJ, Blinder P, Cauwenberghs G, Shih AY & Kleinfeld D Rapid determination of particle velocity from space-time images using the Radon transform. J Comput Neurosci 29, 5–11, doi: 10.1007/s10827-009-0159-1 (2010). [PubMed: 19459038]
14. Kleinfeld D, Mitra PP, Helmchen F & Denk W Fluctuations and stimulus-induced changes in blood flow observed in individual capillaries in layers 2 through 4 of rat neocortex. Proc Natl Acad Sci U S A 95, 15741–15746 (1998). [PubMed: 9861040]
15. Villringer A et al. Confocal laser microscopy to study microcirculation on the rat brain surface in vivo. Brain Res 504, 159–160 (1989). [PubMed: 2598012]
16. Dasari S, Weber P, Makhloufi C, Lopez E & Forestier CL Intravital Microscopy Imaging of the Liver following Leishmania Infection: An Assessment of Hepatic Hemodynamics. J Vis Exp, e52303, doi:10.3791/52303 (2015). [PubMed: 26273959]
17. Hoshikawa R et al. Dynamic Flow Velocity Mapping from Fluorescent Dye Transit Times in the Brain Surface Microcirculation of Anesthetized Rats and Mice. Microcirculation 23, 416–425, doi: 10.1111/micc.12285 (2016). [PubMed: 27113780]
18. Kamoun WS et al. Simultaneous measurement of RBC velocity, flux, hematocrit and shear rate in vascular networks. Nat Methods 7, 655–660, doi:10.1038/nmeth.1475 (2010). [PubMed: 20581828]
19. Sironi L et al. In vivo flow mapping in complex vessel networks by single image correlation. Sci Rep 4, 7341, doi:10.1038/srep07341 (2014). [PubMed: 25475129]
20. Guimaraes P et al. Measuring blood flow velocity from intravital video recordings. Conf Proc IEEE Eng Med Biol Soc 2015, 6289–6292, doi:10.1109/EMBC.2015.7319830 (2015). [PubMed: 26737730]
21. Fontanella AN et al. Quantitative mapping of hemodynamics in the lung, brain, and dorsal window chamber-grown tumors using a novel, automated algorithm. Microcirculation 20, 724–735, doi: 10.1111/micc.12072 (2013). [PubMed: 23781901]
22. Hanna G et al. Automated measurement of blood flow velocity and direction and hemoglobin oxygen saturation in the rat lung using intravital microscopy. Am J Physiol Lung Cell Mol Physiol 304, L86–91, doi:10.1152/ajplung.00178.2012 (2013). [PubMed: 23161885]
23. Fieramonti L et al. Quantitative measurement of blood velocity in zebrafish with optical vector field tomography. J Biophotonics 8, 52–59, doi:10.1002/jbio.201300162 (2015). [PubMed: 24339189]

24. Ellis CG, Ellsworth ML, Pittman RN & Burgess WL Application of image analysis for evaluation of red blood cell dynamics in capillaries. Microvasc Res 44, 214–225 (1992). [PubMed: 1474928]

25. Fraser GM, Milkovich S, Goldman D & Ellis CG Mapping 3-D functional capillary geometry in rat skeletal muscle in vivo. Am J Physiol Heart Circ Physiol 302, H654–664, doi:10.1152/ajpheart.01185.2010 (2012). [PubMed: 22140042]

26. Japee SA, Pittman RN & Ellis CG Automated method for tracking individual red blood cells within capillaries to compute velocity and oxygen saturation. Microcirculation 12, 507–515, doi:10.1080/10739680591003341 (2005). [PubMed: 16147467]

27. Mickoleit M et al. High-resolution reconstruction of the beating zebrafish heart. Nat Methods 11, 919–922, doi:10.1038/nmeth.3037 (2014). [PubMed: 25042787]

Highlights

STAFF simplifies converting capillary flow movie data into quantitative data.

The STAFF macro toolset is implemented in FIJI ImageJ.

Color coded velocity map movie output enables intuitive data exploration.

Spreadsheet output enables further quantitative analyses.

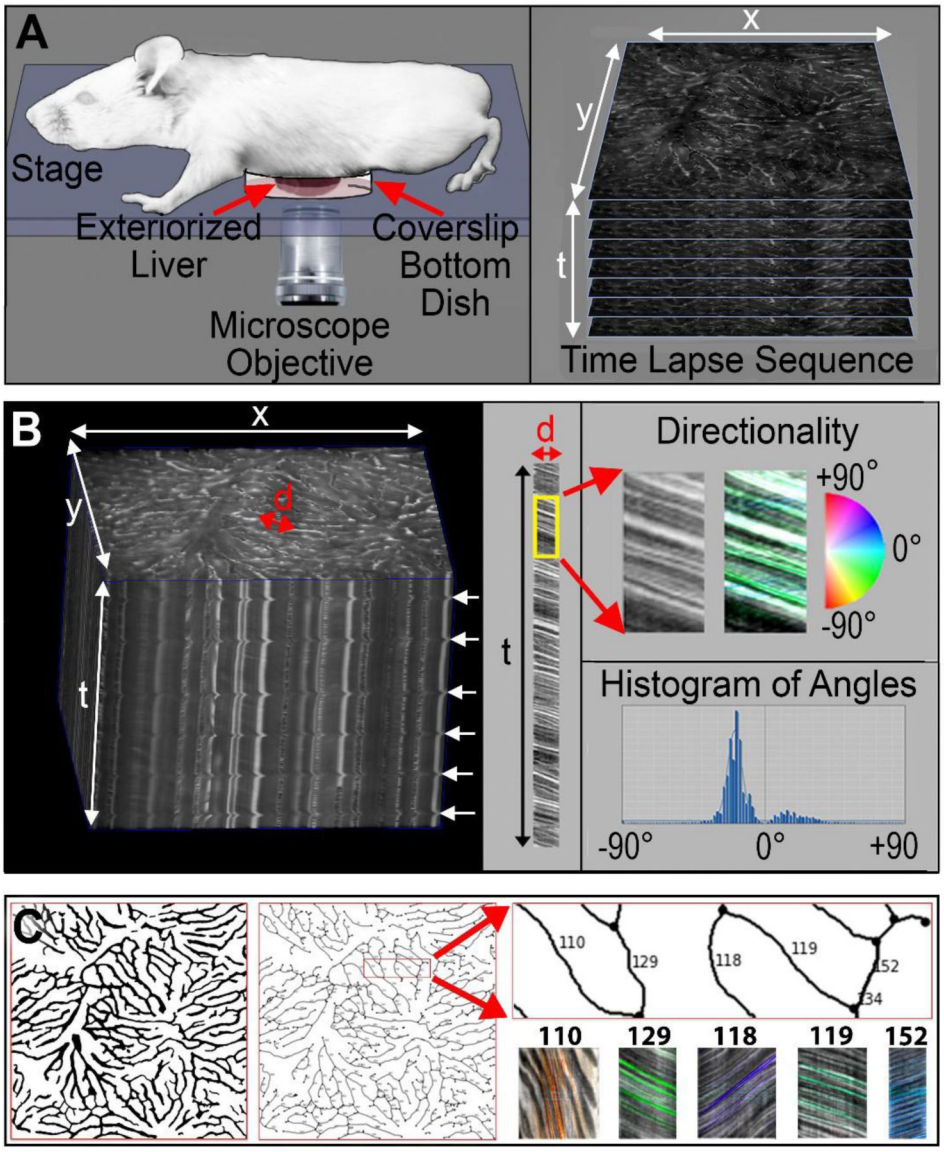

Figure 1. STAFF analysis of microvascular flow.

a, Schematic diagram of the process of time lapse imaging of the liver of a living mouse on the stage of an inverted microscope system. The surgically exposed liver is placed onto the glass coverslip of a 40 mm coverslip bottomed dish, which is then mounted on the warmed stage of an inverted epifluorescence microscope system. Epifluorescence images are then collected at ~100 fps using a high-speed CMOS detector. **b,** The resulting time series displayed as a three-dimensional volume, in which time is the third dimension. The volume shows that the field is stable, except during respirations which are indicated with arrows. RBC velocity measurements are determined for each vessel segment for each inter-respiratory interval based upon the predominant angle in the kymograph. **c,** Measurements of RBC velocities for all vascular segments are obtained from kymographs obtained from line segments throughout the volume. In this example, a semi-automated method was used to generate a “skeleton” of all vascular segments, whose nodes are then identified and used to

distinguish individual segments for quantification. Identifying numbers are associated with each segment in both a map and in the output spreadsheet data file to support inspection and evaluation of individual segment results.

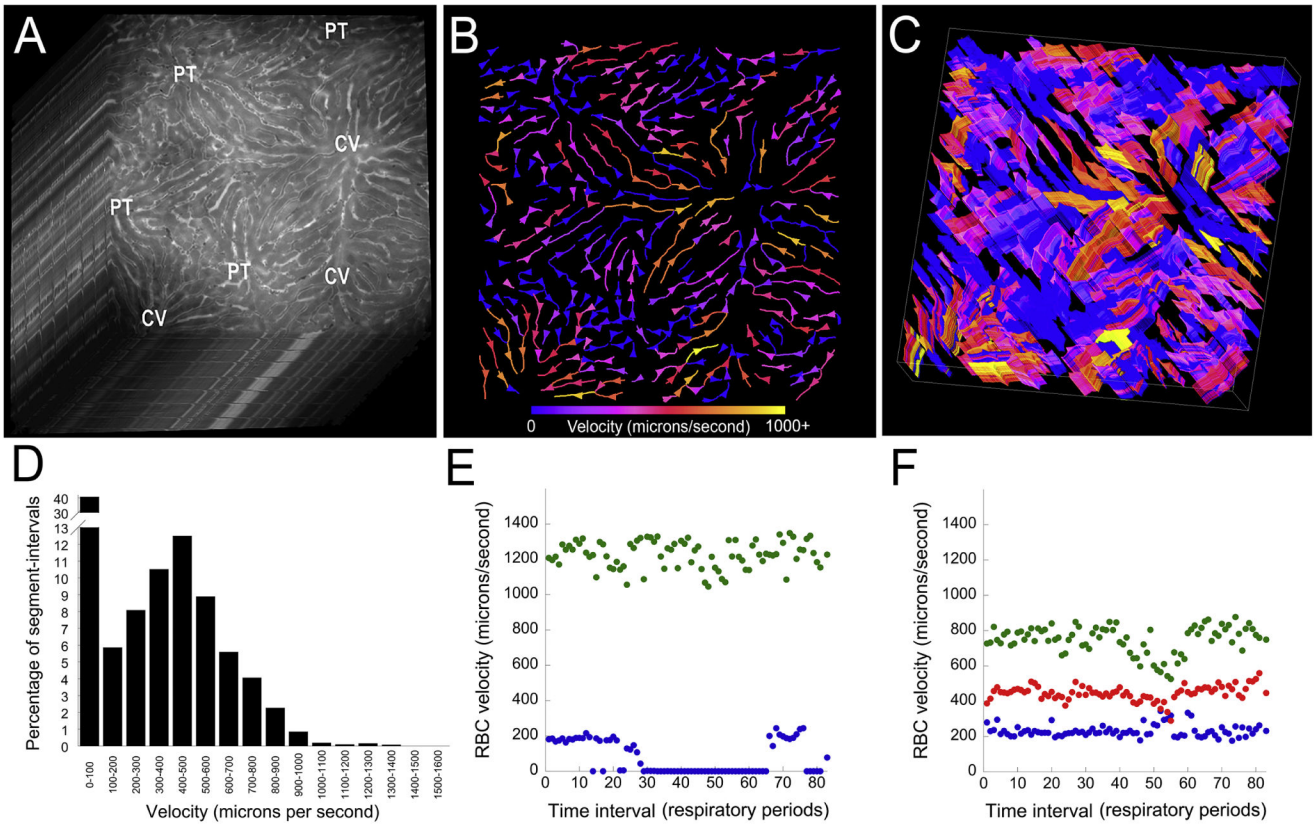

Figure 2. Measurement of RBC velocity in the microvasculature of the mouse liver.

High-speed video microscopy was used to collect images of microvascular flow in the liver of a living mouse at the rate of 97.5 fps, following IV injection of fluorescein-dextran. **a**, Volume rendering of the first twenty seconds of the time series, with time depicted as depth in the volume. CV, central veins; PT, portal triads. Field is 663 microns across. A ten second sample of the time series is presented in Video1, which plays at approximately $1/3_{rd}$ actual speed. **b,** Image depicting RBC velocities during one inter-respiratory interval. Velocities are encoded as colors according to the color bar at the bottom of the image. The time series of the velocities obtained for each of the 81 inter-respiratory period is presented in Video2. **c.** Volume rendering of the RBC velocities over the 81 inter-respiratory periods, with time depicted as depth in the volume. **d.** Histogram of RBC velocities obtained from all segments, over all time intervals. (Note the break in the y-axis). **e.** Examples of RBC velocities plotted as a function of interval number (approximately 2 seconds apart) obtained from a segment with a high RBC velocity and from a segment experiencing intermittent flow stoppages. **f.** Example RBC velocity traces of two segments (red and blue) that merge together upstream of a third segment (green).

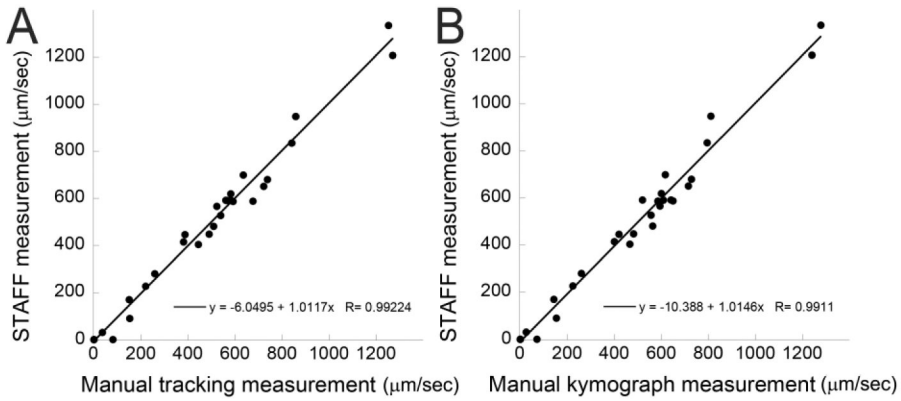

Figure 3. Validation of STAFF measurements.

Measurements of RBC velocity obtained from 33 segments over the first time interval of the dataset shown in Figure 2 were compared to measurements obtained by either **a,** manual tracking of individual cells or **b,** manual measurement of kymograph angles. STAFF measurements agreed well with results provided by either manual technique in both correlation and in having slopes within 2% of unity.

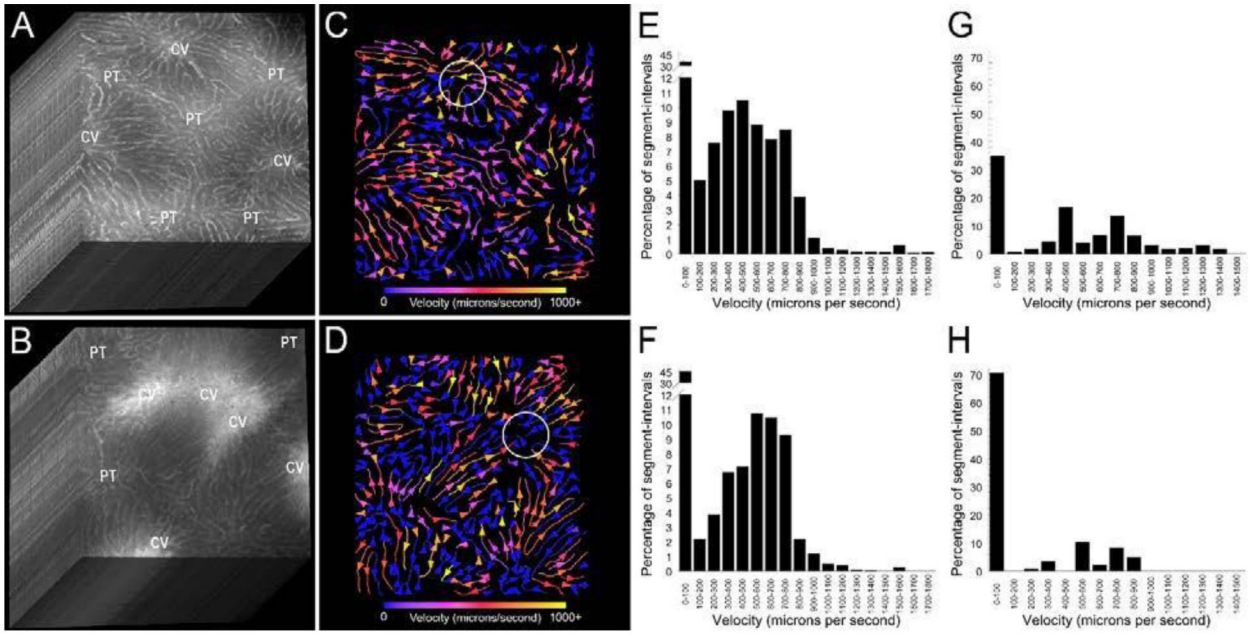

Figure 4. STAFF analysis of effects of acetaminophen on microvascular flow in the mouse liver.

High-speed video microscopy was used to collect time series images of microvascular flow in the livers of living mice 4 hours after intraperitoneal injection of either 250 mg/kg acetaminophen or vehicle. **a. and b.** Volume renderings of the first twenty seconds of the time series (time depicted as depth) for vehicle and APAP-treated mice, respectively. CV, central veins; PT, Portal triads. Field is 663 microns across. A five-second sample of the two time series is presented in Video3, which plays at approximately $1/3_{rd}$ actual speed. **c. and d.** Images depicting RBC velocities during one inter-respiratory interval for vehicle and APAP-treated mice, respectively. Velocities are encoded as colors according to the color bar at the bottom of the image. **e. and f.** Histograms of RBC velocities obtained from all segments, over all time intervals for vehicle and APAP-treated mice, respectively. **g. and h.** Histograms of RBC velocities obtained from the pericentral regions circled in images c. and d., over all time intervals for vehicle and APAP-treated mice, respectively.